COPEDEC VII, 2008, Dubai, UAE

Paper No: 096

ESTIMATION OF BED PROTECTION DAMAGE USING NUMERICAL FLOW MODELLING

by

Nguyen Thanh Hoan[1], Rob Booij[2], Bas Hofland[3], Marcel J.F. Stive[4] and Henk Jan Verhagen[5]

ABSTRACT

The current research is aimed at evaluating the applicability of a numerical flow model to predict bed damage. First, an experimental study was carried out to get more inside into the relation between flow forces acting on a bed and the bed response (damage). The experiments were then used as the basis for the evaluation. Second, the flow was modeled using Deft incompressible flow solver developed at Delft University of Technology. Comparison between measurements and calculations of the flow fields shows a good agreement. The velocity distribution is reproduced very well while in most cases the turbulence intensity is underestimated in the bottom region. The measured and calculated stability parameters are in good agreement (error within $\pm 10\%$) though. The calculated bed damage (dimensionless entrainment rate, Φ_E) has larger error (within $\pm 50\%$) due to its high sensitivity to the value of the stability parameters. However, this is reasonably good for bed damage prediction as the measurement of Φ_E already has an error within $\pm 100\%$ compared to its mean value.

1. INTRODUCTION

Bed protections, often composed of graded rock, are used to prevent bottom erosion and scour development near hydraulic structures. The stones need to be heavy enough to withstand the flow forces. As protected areas are large and large stones are not always easily available, the cost of bed protections is high. Thus a good prediction of stone sizes and weights to be used in the bed protection is needed.

The Shields (1936) formula was developed for uniform flow conditions and is widely used to determine the required stone sizes. In the Shields formula, the near-bed shear stress is the only quantity representing the flow forces on the bed. Previous research has shown that not only the near-bed shear stress (or mean velocity) but also the turbulence influences the stability of the bed material in flowing water. Therefore, it is important to take turbulence effects into account, especially for the design of bed protection near hydraulic structures. At the moment, most design approaches are based on the stability criterion by Shields and can only be used as a rule-of-thumb. Thus, often a physical model is necessary for the design of bed protections in non-uniform flow.

As the capabilities of numerical flow models have been improved significantly, the use of such models to predict bed damage becomes interesting. This would make the use of expensive scale models obsolete. However, to be able to use the outputs of numerical flow models to predict bed damage a proper relation between flow forces acting on the bed (Ψ) and bed response (Φ) is needed.

$$\Phi = f(\Psi) \tag{1}$$

[1] Corresponding author, MSc, Hanoi University of Civil Engineering, 55 Giai Phong street, Hanoi, Vietnam; Present address: PhD student, Delft University of Technology, Faculty of Civil Engineering and Geosciences, Section of Hydraulic Engineering, P.O. Box 5048, 2600 GA Delft, The Netherlands, H.T.Nguyen@TUDelft.NL

[2] Assistant Professor, Delft University of Technology, Faculty of Civil Engineering and Geosciences, Environmental Fluid Mechanics section, P.O. Box 5048, 2600 GA Delft, The Netherlands, R.Booij@TUDelf.NL

[3] Researcher, WL | Delft Hydraulics, Delft, The Netherlands, Bas.Hofland@WLDelft.NL

[4] Professor, Delft University of Technology, Faculty of Civil Engineering and Geosciences, Section of Hydraulic Engineering, P.O. Box 5048, 2600 GA Delft, The Netherlands, M.J.F.Stive@TUDelft.NL

[5] Associate Professor, Delft University of Technology, Faculty of Civil Engineering and Geosciences, Section of Hydraulic Engineering, P.O. Box 5048, 2600 GA Delft, The Netherlands, H.J.Verhagen@TUDelft.NL

This cause-and-effect relation can be obtained from experimental study. In the next section, a brief summary of our experimental study is presented. The experimental results are then used as the basis for evaluating the use of numerical flow models to predict bed damage.

2. BACKGROUND OF THE STONE STABILITY AND EXPERIMENTAL RESULTS

Background of the stone stability

Relation (1) has been established for uniform flow by Paintal (1971) where the Shields stability parameter (Ψ_S) is used to represent the flow forces and the dimensionless bed load transport (Φ_q) is used as bed damage indicator:

$$\Phi_q = 6.56\times10^{18}\Psi_s^{16} \quad \text{for} \quad 0.02 < \Psi_s < 0.05 \tag{2}$$

The Shields stability parameter is expressed as:

$$\Psi_s = \frac{u_*^2}{\Delta g d} \tag{3}$$

where u_* is the shear velocity, Δ represents the specific submerged density of stone ($=(\rho_s-\rho)/\rho$), ρ_s is the density of stone, ρ is the density of water, g is the gravitational acceleration, and d denotes the stone diameter. The dimensionless bed load transport is expressed as:

$$\Phi_q = q/\sqrt{\Delta g d^3};\ \text{where}\ q = \frac{nd^3}{BT} \tag{4}$$

where *n* is the number of stones transported through a cross-section in time *T* and *B* is the section width. Though have been widely used for the design of bed protection, relation (2) is not valid for non-uniform flows because:

i) The use of the Shields stability parameter is not sufficient as the non-uniform turbulence effect is not taken into account.

ii) Bed load transport is dependent on the hydraulics upstream; all the stones passing a certain cross section (i.e., the transport) have been entrained upstream of this section. Bed load transport is therefore considered as non-local parameter. In all cases, stability parameters are local parameters, making Eq. (1) a relation of local and non-local parameters. Such kind of relation can only be valid for uniform flow where along the channel the flow condition is unchanged.

For non-uniform flow Hofland (2005) points out that the dimensionless entrainment rate (Φ_E) should be used as bed damage indicator because it is completely dependent on the local hydrodynamic parameters.

$$\Phi_E = E/\Delta g d \tag{5}$$

where the entrainment rate E is the number of pick-ups (n) per unit time (T) and area (A), $E = nd^3/AT$. Concerning the flow forces acting on the bed, instead of using the Shields stability parameter, the two following alternatives were considered: i) Jongeling et al. (2003) stability parameter:

$$\Psi_{WL} = \frac{\left\langle \left(\bar{u} + \alpha\sqrt{k}\right)^2 \right\rangle_{hm}}{\Delta g d} \tag{6}$$

where k denotes the turbulence kinetic energy, $\alpha = 6$ is an empirical parameter, $\langle ... \rangle_{hm}$ is a spatial average over a distance of hm above the bed, $hm = 5d + 0.2h$ and h is the water depth. ii) Hofland (2005) proposed a stability parameter in which the maximum over the depth of the local values of $(\bar{u} + \alpha\sqrt{k})$ weighted with the relative distance Lm/z is used. The stability parameter, Ψ_{Lm}, is expressed as ($\alpha = 6$):

$$\Psi_{Lm} = \frac{\max\left[\left\langle \bar{u} + \alpha\sqrt{k} \right\rangle_{Lm} \frac{L_m}{z}\right]^2}{\Delta g d} \tag{7}$$

where L_m denotes the Bakhmetev mixing length (κz√(1-z/h)), $\langle ... \rangle_{Lm}$ is a moving average with varying filter length L_m, and z is the distance from the bed. These two stability parameters need to be verified because they were developed based on the limited data set and a large scatter is present in the $\Phi_E - \Psi_{WL}$ and $\Phi_E - \Psi_{Lm}$ relations. Our experimental study focuses on the evaluation of the three aforementioned stability parameters and on the formulation of relation (1) for non-uniform flow.

Experiments

The experiment was carried out in a laboratory open-channel flume with an effective length of 13.30 m and an available width of 0.495 m. An expansion was made near the end of the flume. To this end, the first part of the flume was narrowed at both sides. Then the extension was made by gradually increasing the width from the first segment to the width of the flume. By changing the expansion length (expansion angle), different combinations of velocity and turbulence were obtained. Three different set-ups with expansion angles of 3, 5 and 7 degrees were built.

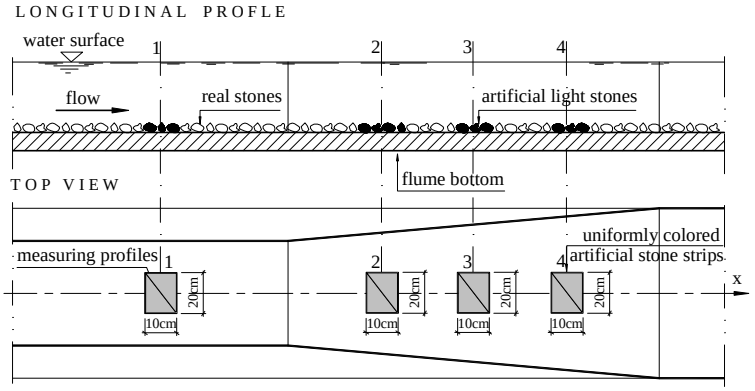

Figure 1: The first experimental set-up with indication of the placement of uniformly colored artificial stone strips (not to scale)

Figure 1 shows a schematic representation of the first experimental set-up. Natural stones having a nominal diameter d_{n50} of 0.80 cm and d_{n85}/d_{n15} of 1.27 were used to create a 4-cm-thick rough bottom. These stones are practically unmovable under the experimental flow conditions. To examine the stone stability, two layers of uniformly colored strips of artificial light stones were placed at designated locations (before and along the expansion). These stones are made of epoxy resin having densities in the range of 1320 to 2023 kg/m^3, mimicking shapes and sizes of natural stones. The artificial stones have a nominal diameter d_{n50} of 0.82 cm and d_{n85}/d_{n15} of 1.11.

Set-up 1 (α = 3^0)					Set-up 2 (α = 5^0)					Set-up 3 (α = 7^0)				
	Q	h	Re	Fr		Q	h	Re	Fr		Q	h	Re	Fr
	[l/s]	[cm]	[10^4]	[-]		[l/s]	[cm]	[10^4]	[-]		[l/s]	[cm]	[10^4]	[-]
1AR	22.0	11.7	6.2	0.50	**2AR**	22.0	11.6	6.2	0.51	**3AR**	22.0	12.1	6.2	0.47
1BR	20.0	12.0	5.7	0.44	**2BR**	20.0	12.0	5.7	0.44	**3BR**	20.0	12.0	5.7	0.44
1CR	23.0	13.0	6.5	0.45	**2CR**	23.0	12.8	6.5	0.46	**3CR**	23.0	12.9	6.5	0.45
1DR	26.5	13.9	7.5	0.47	**2DR**	26.5	13.8	7.5	0.47	**3DR**	26.5	13.8	7.5	0.47
1ER	24.0	13.9	6.8	0.42	**2ER**	24.0	13.2	6.8	0.46	**3ER**	24.0	14.1	6.8	0.41
1FR	27.0	15.0	7.6	0.43	**2FR**	27.0	14.4	7.6	0.45	**3FR**	27.0	14.9	7.6	0.43
1GR	31.0	15.7	8.8	0.46	**2GR**	31.0	16.0	8.8	0.44	**3GR**	31.0	15.7	8.8	0.46
1HR	28.0	15.8	7.9	0.41	**2HR**	28.0	15.9	7.9	0.40	**3HR**	28.0	15.8	7.9	0.41
1IR	31.5	17.0	8.9	0.41	**2IR**	31.5	16.9	8.9	0.41	**3IR**	31.5	16.9	8.9	0.41
1JR	35.5	17.9	10.0	0.43	**2JR**	35.5	17.5	10.0	0.44	**3JR**	35.5	17.5	10.0	0.44
1KR	32.0	18.0	9.1	0.38	**2KR**	32.0	17.8	9.1	0.40	**3KR**	32.0	17.7	9.1	0.39
1LR	35.5	19.0	10.0	0.39	**2LR**	35.5	18.6	10.0	0.41	**3LR**	35.5	18.3	10.0	0.41
										3MR	36.0	12.4	10.2	0.75

Table 1. Summary of hydraulic conditions

Table 1 summarizes all the hydraulic conditions used in the experiment. More detailed descriptions of the experimental set-up, hydraulic conditions, experimental procedures and analysis can be found in Hoan et al. (2007). The results are summarized as follows: i) the experiments indicate that the Shields stability parameter is not sufficient for representing the flow forces acting on the bed in non-uniform flow; ii) Jongeling *et al*. (Ψ_{WL}) and Hofland (Ψ_{Lm}) stability parameters properly represent the flow forces on the bed and these parameters can be successfully used to predict bed damage. Based on the experimental data, relation (1) has been established for both Jongeling *et al.* (2003) and Hofland (2005) stability parameters (see Eqs (8) and (9) and Figure 2). α = 3.5 (for Ψ_{WL}) and α = 3.0 (for Ψ_{Lm}) give the best correlation to the measured entrainment rate. iii) the results confirm the strong influence of the velocity and turbulence intensity distributions on the stability of bed material.

$$\Phi_E = 1.16\times10^{-12}\Psi_{WL}^{4.57} \quad \text{for} \quad 10 < \Psi_{WL} < 25 \;\; (R^2 = 0.82,\ \alpha = 3.5) \tag{8}$$

$$\Phi_E = 1.9\times10^{-8}\Psi_{Lm}^{4.32} \quad \text{for} \quad 1.3 < \Psi_{Lm} < 3.2 \;\; (R^2 = 0.81,\ \alpha = 3) \tag{9}$$

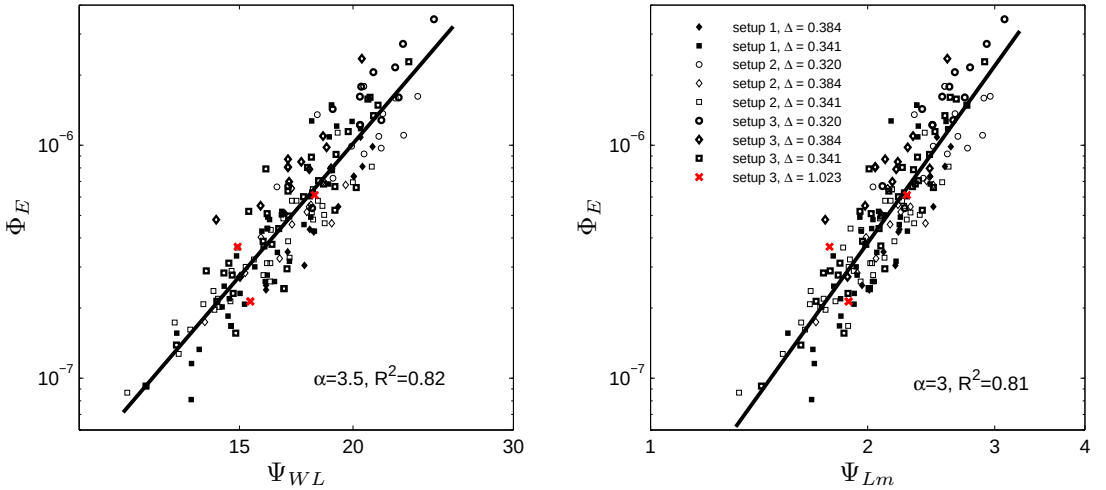

Figure 2: Left: measured Ψ_{WL} versus measured Φ_E. Right: measured Ψ_{Lm} versus measured Φ_E

3. TURBULENCE MODELLING

The experiments have shown that the flow forces acting on the bed and the bed damage have a strong correlation. These relations have been established in the form of Eqs. (8) and (9). Those relations can be used to predict bed damage as long as we know the velocity and turbulence distributions of the flow. In this paper, we utilize a navier stokes solver with *k-ε* turbulence model to simulate the flow in the experiments. The outputs can be used to determine the stability parameters and the bed damage. The aim is to judge the applicability of numerical computation.

Mean flow equation

The flow of an incompressible, viscous Newtonian fluid can be described by a system of flow equations consisting of a continuity equation

$$\frac{\partial u_i}{\partial x_i} = 0 \tag{10}$$

and three momentum equations, the so-called Navier Stokes equations

$$\frac{\partial u_i}{\partial t} + u_j\frac{\partial u_i}{\partial x_j} = -\frac{1}{\rho}\frac{\partial p}{\partial x_i} + \nu\frac{\partial^2 u_i}{\partial x_j^2} + f_i \tag{11}$$

where t is time, x_i are spatial coordinates, u_i are components of the velocity vector, f_i are components of an external force per unit mass, p is the pressure, ρ is the fluid density and ν is the kinematic viscosity. Additional information of this set of flow equations can be found in Rodi (1993). It

is in principal possible to solve this set of equations if we know the boundary conditions and the initial conditions. However, solving these equations for general turbulent flows requires a very fine computational time- and space-grid to resolve all the scales present in the turbulence motion. These requirements are still far beyond the capacity of the modern computer in term of storage and computational time.

Engineers are usually not interested in the details of the fluctuating motion, but in the mean flow field. Therefore a statistical approach can be used in which the Navier Stokes equations are simplified by separating the turbulent flow into a mean ($\overline{u}_i$, $\overline{p}$) and a fluctuating part (u_i', p') and restricting the analysis to time-averages of the turbulent motion.

$$u_i = \overline{u}_i + u'_i, \qquad p = \overline{p} + p' \tag{12}$$

This is called 'Reynolds decomposition'. The mean quantities are defined as

$$\overline{u}_i = \frac{1}{T}\int_0^T u_i dt, \qquad \overline{p} = \frac{1}{T}\int_0^T p_i dt \tag{13}$$

where the averaging time T must be sufficiently large (compared with the time scale of the turbulent motion) for the average value to approach the real time-independent mean value. Substituting Eq. (12) into Eqs. (10) and (11) and subsequent averaging leads to a system of equations for the mean motion. For brevity, the overbars indicating averaged values will be dropped from u_i and p from here on.

The mean continuity equation is as follows

$$\frac{\partial u_i}{\partial x_i} = 0 \tag{14}$$

And the mean momentum equations are

$$\frac{\partial u_i}{\partial t} + u_j \frac{\partial u_i}{\partial x_j} = -\frac{1}{\rho}\frac{\partial p}{\partial x_i} + \nu \frac{\partial^2 u_i}{\partial x_j^2} - \frac{\partial \overline{u'_i u'_j}}{\partial x_j} + f_i \tag{15}$$

The $-\overline{u'_i u'_j}$ terms represent the contribution of the turbulent motion to the mean stress. The turbulent stresses $-\rho\overline{u'_i u'_j}$ are called the *Reynolds stresses*. The process of averaging has introduced unknown terms representing the transport of mean momentum by turbulent motion. Consequently, this set of equations cannot be solved without additional information. This is known as the *closure problem of turbulence*. It has led to the development of turbulence models, in which the Reynolds stresses are *modeled*. An extensive review of turbulence models and their application in hydraulics can be found in Rodi (1993). In this research the standard two-equation $k-\varepsilon$ model was chosen as it is widely tested and used for hydraulic flow problems. The $k-\varepsilon$ model employs conservation equations for the rate of turbulent kinetic energy k and for the rate of energy dissipation ε. In the next section, the $k-\varepsilon$ model will be described in somewhat more detail.

The standard two equation k-ε model

In the standard two-equation $k-\varepsilon$ model, two extra transport equations are introduced to represent the turbulent properties of the flow.

For turbulent kinetic energy:

$$\frac{\partial k}{\partial t} + \frac{\partial}{\partial x_i}(k u_i) = \frac{\partial}{\partial x_i}\left[\left(\nu + \frac{\nu_t}{\sigma_k}\right)\frac{\partial k}{\partial x_i}\right] + P_k - \varepsilon \tag{16}$$

For turbulent dissipation:

$$\frac{\partial \varepsilon}{\partial t} + \frac{\partial}{\partial x_i}(\varepsilon u_i) = \frac{\partial}{\partial x_i}\left[\left(\nu + \frac{\nu_t}{\sigma_k}\right)\frac{\partial \varepsilon}{\partial x_i}\right] + c_{1\varepsilon}\frac{\varepsilon}{k}P_k - c_{2\varepsilon}\frac{\varepsilon^2}{k} \tag{17}$$

where ε is the turbulent dissipation that determines the scale of the turbulence, k is the turbulent kinetic energy that determines the energy in the turbulence, P_k is the production rate of turbulent energy given by:

$$P_k = -\overline{u'_i u'_j}\frac{\partial u_i}{\partial x_j} \tag{18}$$

The eddy viscosity is modeled as:

$$\nu_t = c_\mu \frac{k^2}{\varepsilon} \tag{19}$$

The model contains some closure constants which are given as follows:

- For standard $k-\varepsilon$ model:

$$c_\mu = 0.09,\ \ c_{1\varepsilon} = 1.44,\ \ c_{2\varepsilon} = 1.92,\ \ \sigma_k = 1.0,\ \ \sigma_\varepsilon = 1.3 \tag{20}$$

- For RNG $k-\varepsilon$ model:

$$c_\mu = 0.085,\ \ c_{1\varepsilon} = 1.42,\ \ c_{2\varepsilon} = 1.68,\ \ \sigma_k = 0.7179,\ \ \sigma_\varepsilon = 0.7179 \tag{21}$$

4. NUMERICAL MODEL

The turbulent flows through the flume have been simulated using Deft (formerly known as ISNaS - Information System for Navier-Stokes equations) incompressible flow solver developed at Delft University of Technology. With the Deft code it is possible to compute complex turbulent flows in two or three dimensions. The applicability of the model for predicting bed damage was investigated by running the model with input that was based on the experiments. Since we are mainly interested in the output which is then used as input to predict bed damage, we focus on the velocity and turbulence profiles. In order to asses the model results properly, we will compare the model results (i.e., velocity and turbulence distributions) with the results of these experiments. The deviation of the simulated flow field from the measurements resulted in the differences between the calculated and measured bed damage. This is evaluated in the next section.

The Deft code has implemented different turbulence models, among others the standard $k-\varepsilon$ model and RNG $k-\varepsilon$ model. Both turbulence models were employed in the early state of modeling process. The turbulence model that gives better results was then used for all simulations.

Due to the symmetry, only one half of the flume needs to be considered. The inlet profiles for the velocity and turbulence quantities can be regarded as uniform distributions. This close-to-the-experimental-condition assumption was employed in the validation simulation. Because the velocity distribution approaches to logarithmic (or parabolic) form along the flume, to speed up the computation a parabolic velocity distribution was assumed at the inlet. In this case, the velocity distribution has the following form:

$$u(z) = az^2 \tag{22}$$

where a is a constant. The discharge (Q) at the flume entrance can then be determined as

$$Q = \int_0^h Bu(z)dz = B\int_0^h az^2 dz = B\frac{ah^3}{3} \tag{23}$$

where B is the flume width at the inlet and h is the water depth. From Eq. (23) one has

$$a = \frac{3Q}{Bh^3} \tag{24}$$

Thus, velocity distribution at the inlet can be expressed as:

$$u(z) = \frac{3Qz^2}{Bh^3} \tag{25}$$

This inlet condition is prescribed in routine *usfund.f*. The flow at the end of the flume is described as *outflow* in Deft which prescribes the least restrictive outflow boundary condition, viz. stress equals zero at the boundary. In this case the boundary condition can be interpreted as pressure zero and no

restriction to the tangential velocity component. The flume bottom is described as a rough surface. As the roughness influences both the velocity and turbulence distributions, special attention was paid to choose a correct modeling of the bottom roughness in the calibration simulation. The free water surface was modeled as a rigid lid with free-slip conditions. The flume side wall was modeled as smooth wall in the validation simulation. In the calibration step different roughness values were applied to the side wall to gain a better velocity distribution. In the numerical model, the middle of the flume becomes a symmetric boundary condition where normal component of the velocity is zero and the shear stress is zero.

The mesh of the numerical model was made using a structured grid with refinement in regions where steep velocity gradients occur. The grid size in flow direction (Δx) gradually decreases from approx. 0.11m to 0.03m in the first straight part of the flume[6]. The grid size Δx of approx. 0.029m is unchanged along the expansion. The number of cells in vertical direction (z) is 10. The grid size Δz gradually increases from the bottom to the surface in a way that the last cell is 2 times the first cell. The number of cells in transverse direction (y) is 8, resulting in a grid size Δy of approx. 0.031m. Figure 3 shows the sketch of the domain configuration. Boundary S1, S2, S3 represent the flume bottom. Surface S4, S5, S6 represent the flume side wall. Surface S8, S9, S10 represent the vertical symmetric plan of the flume. Surface S12, S13, S14 model the free surface with free-slip condition. The flume inlet and outlet are represented by surface S11 and S7, respectively.

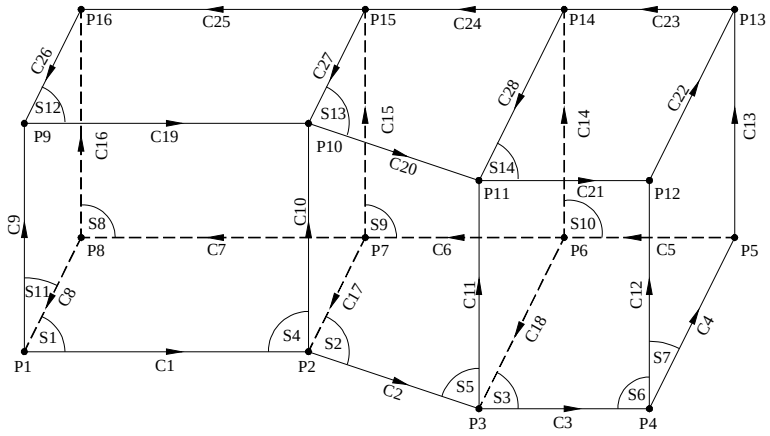

Figure 3: Definition region of the model set-up.

Model validation

In the validation state the simulation computation was made without any tuning of model coefficients. The bottom roughness was described as it is, i.e., ks = 0.008m (stone diameter). The velocity and turbulence are uniformly distributed at the inlet. The side wall was smooth. The free surface was modeled as a rigid lid with free-slip condition. The flow at the end of the flume was modeled as *outflow*. The flume middle was modeled as symmetric boundary condition. Both standard $k-\varepsilon$ and RNG $k-\varepsilon$ turbulence models were employed. In the validation run, different time-step Δt and end time t_{end} were tried. The time-step must satisfy the Courant condition (Wilcox, 1994):

$$\frac{\Delta t}{\Delta l}u<1 \qquad (26)$$

with Δl as grid size in flow direction. After several trials, a time-step Δt of 0.008s was chosen. In all cases the computation converged at an end time less than 20s. In the computation, an end time t_{end} of 30s was chosen, ensuring that the computation was ended by convergence criterion. Figure 4 shows the computational results with the standard $k-\varepsilon$ model.

[6] The length of this part is 7.6m (set-up 1) and 8.2m (set-up 2 and 3).

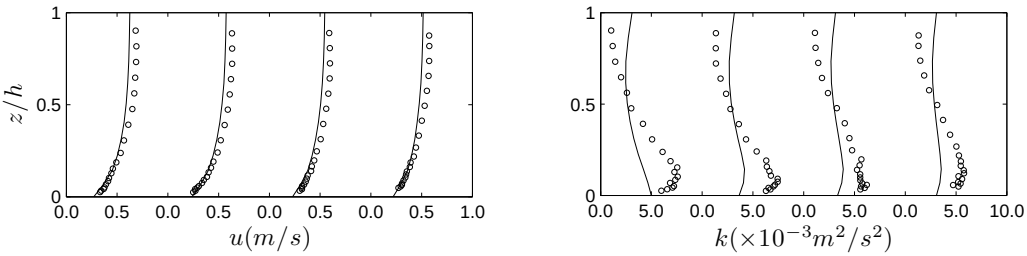

Figure 4: Profiles of calculated (lines) and measured (circles) flow parameters over the flume with flow condition 1AR (see Table 1). The results at profile 1 to 4 are plotted from left to right. See Fig. 1 and Hoan *et al.* (2007) for more information on the measuring profile location.

It turns out that the standard $k-\varepsilon$ and RNG $k-\varepsilon$ turbulence models give similar results. Velocity distributions were predicted fairly well compared to the measured data. However, in the upper region ($z/h>0.5$) the velocity is still underestimated. This can be explained by the fact that in reality the side walls are not completely smooth. Thus, the flow concentrates more to the middle region. By adding roughness to the side wall, better velocity distributions are expected. The turbulence intensity in the upper region ($z/h>0.5$) is rather high mainly because of the free-slip condition at the surface. Turbulence is underestimated in the lower region ($z/h<0.4$) but the distribution shows a similar shape as the measurements. In short, the validation simulation showed that the model is able to predict the flow in the flume and suggested what model coefficients and parameters should be tuned in the calibration step.

Model calibration

In the calibration step several flow conditions were chosen to model. Velocity at the inlet was assumed to have a parabolic distribution and is described in Eq. (25). The roughness values of the bottom and side wall were tested systematically. Because the measurements have shown that turbulence kinetic energy near free surface in most cases is approximately 10^{-3} m^2/s^2, this value was used to prescribe turbulence at the free surface in the model. The standard $k-\varepsilon$ and RNG $k-\varepsilon$ turbulence models were also used. Best results in terms of velocity and turbulence distributions can be obtained when the following parameters are used. Bottom roughness $k_s=0.02m$ (i.e., $k_s\sim 2d$ with d is stone diameter), side wall roughness $k_s=0.005m$, the velocity at the free surface is described as free-slip while turbulence kinetic energy $k=10^{-3}m^2/s^2$. With the tuning coefficients, the standard $k-\varepsilon$ and RNG $k-\varepsilon$ turbulence models give similar results. The standard $k-\varepsilon$ model, however, gives little better turbulence results in addition to less computation time. The standard $k-\varepsilon$ model, therefore, was used in all simulations.

Simulation results

In the computation the chosen coefficients in the calibration step were consistently used for all flow conditions. As measurements are available for all flow conditions, calculations and measurements were compared. As the number of flow conditions that was computed is large, only typical results are presented. Figure 5 depicts the calculated and measured profiles of $\bar{u}$ and k for the three set-ups with flow condition A (i.e., 1AR, 2AR, 3AR) as examples of the results of the $k-\varepsilon$ model. The mean flow is calculated rather well while the turbulence intensity is reproduced reasonably. Turbulence intensity is underestimated in the bottom region ($z/h<0.4$). These hold for both the flow in the straight part (profile 1) and the flow along the expansion (profile 2 to 4).

Similar results are also found for the other simulations. In general, the Deft code models the flow very well (both at before and along the expansion). A good flow field calculation is expected to give a good stability parameter calculation. However, a small difference in the values of the stability parameter is enhanced in the resulting damage. This is examined in the next section.

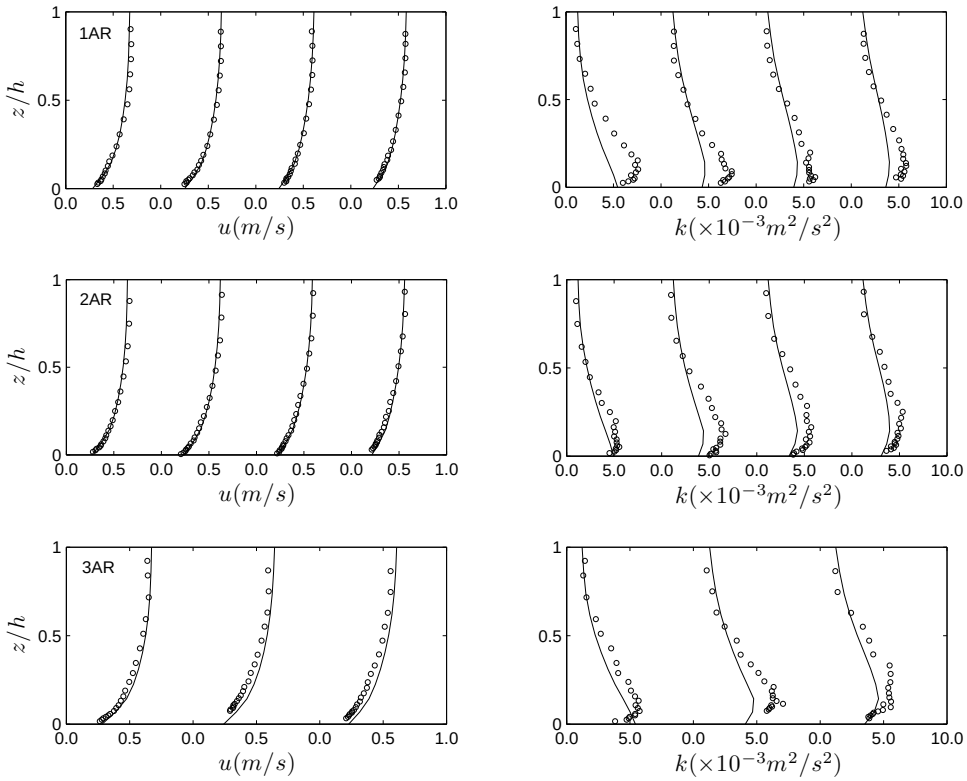

Figure 5: Comparison of calculations (lines) and measurements (circles). From top to bottom: flow condition 1AR, 2AR, 3AR. The results at profile 1 to 4 are plotted from left to right.

5. ESTIMATION OF BED DAMAGE USING THE OUTPUTS OF NUMERICAL FLOW MODELS

The outputs of the numerical flow model are used to calculate the stability parameters as described in Eqs. (6) and (7). Figure 6 compares the calculations and measurements of the key parameters presented in the two stability parameters. Two flow conditions are chosen as typical examples. 2BR is one of the best computations while 2IR is one of the least accurate simulations. In both cases the velocity is modeled well. Turbulence is modeled well for 2BR condition. In contrast, turbulence is underestimated up to 35% for 2IR flow condition. However, in both cases the calculated $\left(\overline{u}+\alpha\sqrt{k}\right)^2$ is in good agreement with the measurements.

Comparison between the calculations and measurements of the stability parameters are depicted in Figure 7. Good agreement is found for both Ψ_{WL} and Ψ_{Lm}. Hofland stability parameter (Ψ_{Lm}) is better calculated while Jongeling *et al*. parameter (Ψ_{WL}) is more underestimated. However, the difference is small and the errors for both parameters are within $\pm 10\%$.

Though good agreement is found for the calculated and measured stability parameters, the calculated Φ_E (bed damage) is expected to have larger errors according to Eqs. (8) and (9) (i.e., a small error in Ψ_{WL} or Ψ_{Lm} can lead to much larger error in Φ_E). Figure 8 shows the comparison between the measured and calculated Φ_E. It shows that the errors are within $\pm 50\%$ which is still good for bed damage prediction; especially when comparing the measured Φ_E to its mean value (i.e., Eqs. (8) and (9)), the errors already have the order of 100% (see Fig 2).

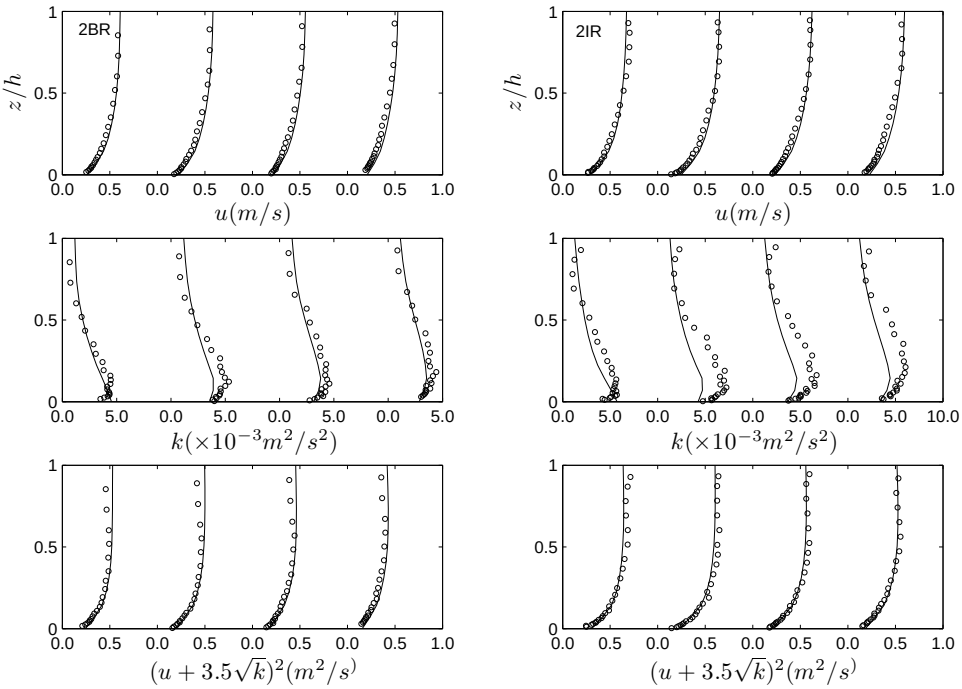

Figrue 6: Vertical distributions of key parameters in Eqs. (6) and (7). Left: flow condition 2BR. Right: flow condition 2IR.

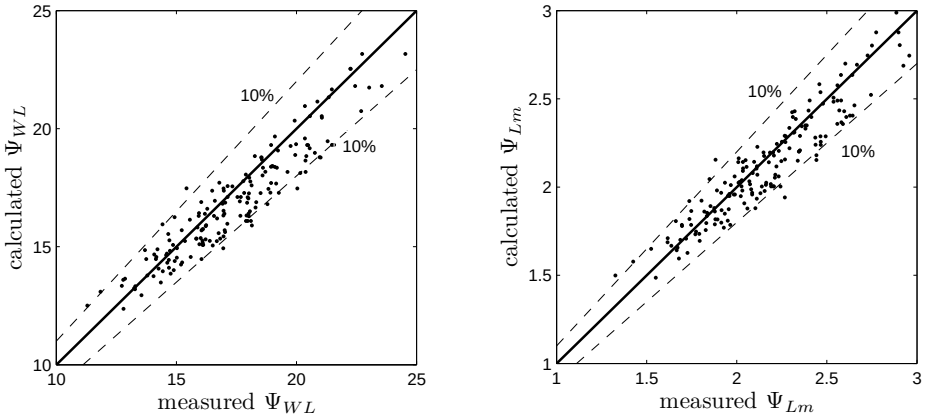

Figrue 7: Comparison of measured and calculated stability parameters.

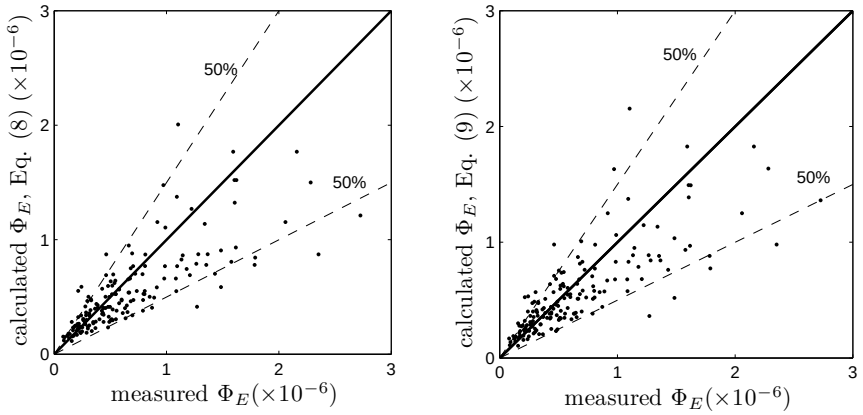

Figrue 8: Comparison of measured and calculated bed damage (Φ_E). The bed damage was calculated using Eq. (8) (left) and Eq. (9) (right).

6. CONCLUSIONS

Systematic comparison between measurements and calculations has shown that the standard $k-\varepsilon$ turbulence model can compute the flow field well. The velocity distribution is reproduced very well while the turbulence intensity is underestimated in the bottom region. The stability parameters can be calculated with error within $\pm 10\%$. The calculated bed damage (dimensionless entrainment rate) has larger errors (within $\pm 50\%$) due to its high sensitivity to the value of the stability parameters. However, this is reasonably good for bed damage prediction as the measurement of Φ_E already has error within $\pm 100\%$ compared to its mean value.

7. ACKNOWLEDGMENT

We would like to express our thanks to Dr. Marcel Zijlema for his valuable advice and assistance in numerical flow modeling using Deft incompressible flow solver. We would like to thank the Fellowship Awards Committee of PIANC-COPEDEC VII for awarding us a fellowship to attend the conference.

8. REFERENCES

Hoan, N. T., Booij, R., Hofland, B., Stive, M. J., Verhagen, H. J. (2007). Stone stability under decelerating open-channel flow in a gradual expansion. Coastal Structues 5th International conference. Venice, Italy.

Hofland, B. (2005). Rock & roll: turbulence-induced damage to granular bed protections. Ph.D. thesis, Delft University of Technology.

Jongeling, T.H.G, Blom, A., Jagers, H.R.A, Stolker, C., Verheij, H.J. (2003). *Design method granular protections* (Technical Report Q2933 / Q3018). WL| Delft Hydraulics. (In Dutch)

Paintal, A. S. (1971). Concept of critical shear stress in loose boundary open channels. *Journal of Hydraulic Research,* 9(3), 91-113.

Rodi, W. (1993). *Turbulence models and their applications in hydraulics; a state-of-the-art review*. IAHRMonograph series. Balkema, Rotterdam, 3rd edition.

Shields, A. (1936). *Anwendung der Aehnlichkeitsmechanik und der Turbulenzforschung auf die Geschiebebewegung*. Mitteilungen der Preussischen Versuchsanstalt fur Wasserbau und Schiffbau, Heft 26, Berlin. (in German)

Wilcox, D. C. (1994). *Turbulence modeling for CFD*: DCW Industries.